Functional interplay between NF-κB-inducing kinase and c-Abl kinases limits response to Aurora inhibitors in multiple myeloma

Laura Mazzera,[1,2] Manuela Abeltino,[1] Guerino Lombardi,[2] Anna Maria Cantoni,[3] Roberto Ria,[4] Micaela Ricca,[2] Ilaria Saltarella,[4] Valeria Naponelli,[1] Federica Maria Angela Rizzi,[1,5] Roberto Perris,[5,6] Attilio Corradi,[3] Angelo Vacca,[4] Antonio Bonati[1,5] and Paolo Lunghi[5,6]

[1]Department of Medicine and Surgery, University of Parma, Parma; [2]Istituto Zooprofilattico Sperimentale della Lombardia e dell'Emilia Romagna "Bruno Ubertini," Brescia; [3]Department of Veterinary Science, University of Parma, Parma; [4]Department of Biomedical Sciences and Human Oncology, Section of Internal Medicine and Clinical Oncology, University of Bari "Aldo Moro" Medical School, Bari; [5]Center for Molecular and Translational Oncology, University of Parma, Parma and [6]Department of Chemistry, Life Sciences and Environmental Sustainability, University of Parma, Parma, Italy

 doi:10.3324/haematol.2018.208280

Received: Ocrtober 17, 2018.

Accepted: April 3, 2019.

Pre-published: April 4, 2019.

Correspondence: *PAOLO LUNGHI* - p.lunghi@libero.it

SUPPLEMENTAL INFORMATION FOR: "Functional Interplay between NIK and c-Abl kinases Limits Response to Aurora inhibitors in Multiple Myeloma"

Supplemental Methods

Reagents

For our in vitro experiments, we used three potent and selective small-molecule inhibitors of Aurora A and B kinases: the pan-Aurora kinases inhibitor MK-0457 [1] (Merck & Co., Rahway, NJ), the pan-Aurora kinases inhibitor PHA-680632 [2] (kindly provided by dr. Jürgen Moll, Pfizer/Nerviano, Italy) which has been reported to have both in vitro and in vivo similar activity against the Aurora kinases of its close analog PHA-739358, that is one of the first AKIs to enter the clinic and has been studied in Phase I and II trials [3-5], and AMG-900 [6] (Cayman Cemical Company, Michigan USA). All Pan-AKIs were dissolved in DMSO (200nM stock solution) and stored at -20°C until use. In this study, all the pan-Aurora kinase inhibitors, used at concentrations within the range of clinically achievable levels (0.4μM for MK-0457 [1, 7], 1μM for PHA-680632 [2, 7] and 40nM for AMG-900 [6, 8]), exhibited similar biological and biochemical activities as single agents or in combination with the other inhibitors used in this study.

The NIK inhibitor isoquinoline-1,3(2H,4H)-dione (Santa Cruz Biotechnology, Santa Cruz, CA) was dissolved in DMSO at 200 mM and stored at -20°C until use.

The proteasome inhibitor Bortezomib (PS-341) purchased from Janssen-Cilag (Milan, Italy) was dissolved in sterile water at 0.05 mg/mL and stored at -20°C until use.

The tyrosine kinase inhibitors Imatinib mesylate and Nilotinib provide by Novartis Pharmaceuticals (Basel, Switzerland), were dissolved in distilled water and in DMSO respectively and stored at -20°C until use.

The Pan-PIM kinase inhibitor SMI-4A (5Z)-5-[[3-(Trifluoromethyl) phenyl] methylene]-2,4-thiazolidinedione provided from Sigma-Aldrich (St. Louis, MO), dissolved in DMSO at 20 mg/mL stock solution and stored at -20°C until use.

The STAT3 inhibitor Stattic (6-Nitrobenzo [b]thiophene-1,1-dioxide) provided from Sigma-Aldrich, dissolved in DMSO at 50 mg/mL stock solution and stored at -20°C until use.

Cell Culture

Human Myeloma cell lines (HMCLs) ($2x10^5$ cells/mL), fresh purified MM ($2,5x10^5$ cells/mL) cells and PBMCs ($2,5x10^5$ cells/mL) were seeded in fresh RPMI-1640 medium

(Euroclone, Pero, Milan, Italy), supplemented with 10% fetal bovine serum (FBS) (Sigma-Aldrich), 2mM L-glutamine and penicillin G (100 U/mL)/streptomycin (100mg/mL) (Euroclone). HS-5 cells were grown in DMEM (Sigma-Aldrich) supplemented with 10% FBS, L-glutamine and penicillin G/streptomycin.

Multiple Myeloma cells and Peripheral Blood Mononuclear Cells isolation

Mononuclear cells were isolated from Bone Marrow aspirates by Ficoll density sedimentation after patient informed consent in accordance with the Helsinki Protocol.

The isolation of tumor plasma cells was performed using a MACS separator (Miltenyi Biotec, Germany) with magnetic microbeads coupled to CD138 monoclonal antibody, according to the manufacturer's protocol. Only cell populations with purity greater than 90% monitored by flow cytometry analysis with anti-CD138-PC5 antibodies (Beckman Coulter) were used for experiments.

Peripheral blood mononuclear cells (PBMCs) were obtained by Ficoll-Hypaque density sedimentation of heparinized blood from five healthy volunteers after informed consent in accordance with the Helsinki Protocol.

Co-culture of myeloma cells and HS-5 stromal cells

Co-culture system between MM cells and adherent HS-5 cells was performed in RPMI-1640 medium at 10% FBS. Before the experiments HS-5 cells were plated to confluence and incubated overnight in 6-well or 24-well plates. MM cells ($2x10^5$ cells/mL) were incubated with the NIK inhibitor (NIK-in) at 10 μM, or with the pan-PIM kinase inhibitor (SMI-4a) at 10 μM, or Imatinib at 2 μM or Nilotinib 2 μM for 3 hours in presence or absence of human bone marrow-derived stromal cell line HS-5 in a 5:1 ratio, and then were treated with MK-0457 at 0.4μM or PHA-680632 at 1μM. After the treatments the cells were detached with EDTA 0.05% (Sigma-Aldrich), stained with anti-CD38/CD138-PC5 (Beckman Coulter, Miami, F) and the apoptotic MM cells were determined by flow cytometry as CD38/CD138+ annexin-V+ cells.

RPMI-8226/R5, OMP-2, U266, JJN3 and primary MM cells were seeded in direct contact to HS-5 cells monolayer and after the treatments HMCLs were detached by carefully wash off since they did not firmly adhere to HS-5 cells, and flow cytometry analysis with anti-CD38/CD138-PC5 antibodies (Beckman Coulter) demonstrated that the purity of myeloma cell population after co-culture was over 98%. Since adhering myeloma cells may affect the purity of HS-5 cells harvests even after the washout, we used anti-CD38/CD138 staining to

assay the phenotype of HS-5 cells and less than 5% CD38/CD138+ cells were detected in HS-5 cells harvest after washout. Cell death of MM cells was then monitored by flow cytometry as CD38/CD138+ annexin-V/PI+ cells.

Since RPMI-8226 cells firmly adhere to HS-5 cells, the direct contact co-culture experiments were performed in parallel using a transwell system (Costar, 0.4 μm pore size; Corning, NY) which allowed to test protein expression of non-contaminated MM cells by western blot analysis. To evaluate apoptosis of RPMI-8226 directly adhered to HS-5 cells monolayer, the cells were detached with EDTA 0.05% (Sigma-Aldrich), stained with anti-CD38/CD138 and the apoptotic MM cells were determined by flow cytometry as CD38/CD138+ annexin-V/PI+ cells.

Apoptosis assays

Cytofluorimetric analysis was performed to evaluate the percentage of apoptotic cells by Sub-G1 DNA content and Annexin V-FITC/PI or Annexin V-PE/7-AAD staining.

Enzyme-linked immunosorbent assay

The DNA-binding activity of NF-κB subunits was quantified by the TransAm NF-κB family enzyme-linked immunosorbent assay kit according to the manufacturer's protocols (Active Motif, Rixensart, Belgium).

siRNA transfections

Prior to electroporation OPM-2, U266, RPMI-8226, RPMI-8226/R5 and JJN3 HMCLs were washed twice with serum-free RPMI-1640 medium (Euroclone) and resuspended in Opti-MEM (GibcoBRL, Grand Island, NY) to a final concentration of $24x10^6$ cells/mL. Subsequently, 0.4 mL of cells suspension was mixed either with 10 μg of siRNA against NIK (MISSION® esiRNA human MAP3K14), or TRAF2 (MISSION® esiRNA human TRAF2), or STAT3 (MISSION® esiRNA human STAT3), or PIM2 (MISSION® esiRNA human PIM2), or PIM1 (MISSION® siRNA human PIM1) or non-specific control esiRNA from Sigma-Aldrich.

To silence Aurora kinases expression, HMCLs were transfected with 1nmol of siRNA against Aurora A (003545) and against Aurora B (003326) or non-specific control siRNA (001206), all obtained from Dharmacon Tech, Lafayette, Co. Subsequently HMCLs were electroporated in a 0.4-cm cuvette using the Gene Pulser electroporation apparatus (Bio-Rad Laboratories Inc, Herculex, California) using a single-pulse protocol (voltage 250

mV/capacitance 1050 µF). HMCLs were harvested for Immunoblotting to monitor knockdown protein levels by siRNA 24 and 48 hours after siRNA transfection.

Electroporation of plasmids

RPMI-8226 and RPMI-8226/R5 cells were electroporated with 10 µg of pLenti-CMV-GFP-2A-Puro-Blank Lentiviral Control Vector or with pLenti-GIII-CMV-hMAP3K14-GFP-2A-Puro Lentiviral Vector (Applied Biological Materials Inc, Vancouver, BC, Canada). Both lentviral expression vectors co-expressed GFP to monitor the transfection by flow cytometry. After electroporation cells were expanded in complete medium for three days after which the medium was replaced with selection medium containing 0.6 µg/mL puromycin for selection of stable transfected pools. Up to 95% of GFP-positive cells were obtained. HMCLs stably transfected were continuously cultured under puromycin selection. after growth stabilization, the cells were used in the experiments described.

Antibodies

Primary and secondary antibodies used for western blot, immunohistochemistry and immunofluorescence analysis are listed in the Table:

ANTIBODIES FOR WESTERN BLOT	**SOURSE and #catalogue**
rabbit polyclonal anti-NIK	Cell Signaling Technology #4994
rabbit polyclonal anti-TRAF2	Cell Signaling Technology #4712
rabbit polyclonal anti-TRAF3	Cell Signaling Technology #4729
rabbit monoclonal anti-Aurora A/AIK (1G4)	Cell Signaling Technology #4718
rabbit polyclonal anti-Aurora B/AIM1	Cell Signaling Technology #3094
rabbit monoclonal anti-pospho-IKKα/β (Ser176/180) (16A6)	Cell Signaling Technology #2697
rabbit polyclonal phospho-NF-κB2 p100 (Ser866/870)	Cell Signaling Technology #4810
rabbit monoclonal anti-phospho-IκB-α (Ser32) (14D4)	Cell Signaling Technology #2859
rabbit monoclonal anti-NF-κB p65 (93H1)	Cell Signaling Technology #3033
rabbit polyclonal anti-NF-κB1 p105/p50	Cell Signaling Technology #3035
rabbit polyclonal anti-NF-κB2 p100/p52	Cell Signaling Technology #4882
rabbit polyclonal anti-RelB (C1E4)	Cell Signaling Technology #4922
mouse monoclonal anti-Histone H2B (53H3)	Cell Signaling Technology #2934
rabbit polyclonal anti-phospho-p44/42 ERK (Thr202/Tyr204)	Cell Signaling Technology #9101

rabbit polyclonal anti-p44/p42 ERK	Cell Signaling Technology #9102
rabbit monoclonal anti phospho-STAT3 (Tyr705) (D3A7)	Cell Signaling Technology #9145
Mouse monoclonal anti-STAT3 (124H6)	Cell Signaling Technology #9139
rabbit monoclonal anti phospho-Jak2 (Tyr1007/1008) (C80C3)	Cell Signaling Technology #3776
rabbit monoclonal anti phospho-Src (Tyr416) (D49G4)	Cell Signaling Technology #6943
rabbit monoclonal anti-Src (32G6)	Cell Signaling Technology #2123
rabbit polyclonal anti phospho-c-Abl (Tyr245)	Cell Signaling Technology #2861
rabbit monoclonal anti phospho-c-Abl (Tyr412) (247C7)	Cell Signaling Technology #2865
rabbit polyclonal anti phospho-c-Abl (Thr735)	Cell Signaling Technology #2864
Rabbit monoclonal Phospho-Aurora (Thr288)/Aurora B (Thr232)/Aurora C (Thr198 (D13A11)	Cell Signaling Technology #2914
Rabbit polyclonal anti-cleaved caspase-3 (Asp175)	Cell Signaling Technology #9661
rabbit polyclonal anti-Bcl-xL	Cell Signaling Technology #2762
rabbit polyclonal anti-A1/Bfl-1	Cell Signaling Technology#4647
rabbit polyclonal anti-Mcl-1	Cell Signaling Technology #4572
rabbit polyclonal anti-XIAP	Cell Signaling Technology #2042
rabbit polyclonal anti phospho-Bad (Ser112)	Cell Signaling Technology #9291
rabbit monoclonal anti-Histone H3 (3H1)	Cell Signaling Technology #9717
mouse monoclonal anti-β Tubulin (D-10)	Santa Cruz Biotechnology sc-5274
rabbit polyclonal anti phospho-STAT3 (Ser727)-R	Santa Cruz Biotechnology sc-8001-R
mouse monoclonal anti phospho-STAT3 (Tyr705) (B-7)	Santa Cruz Biotechnology sc-8059
Mouse monoclonal anti-Jak2 (D-2)	Santa Cruz Biotechnology sc-7345
Mouse monoclonal anti-NIK (A-12)	Santa Cruz Biotechnology sc-8417
mouse monoclonal anti-c-Abl (24-11)	Santa Cruz Biotechnology sc-23
Mouse monoclonal anti-PARP (F12)	Santa Cruz Biotechnology sc-8007
mouse monoclonal anti-PIM2 (1D12)	Santa Cruz Biotechnology sc-13514
mouse monoclonal anti-PIM1 (12H8)	Santa Cruz Biotechnology sc-13513
mouse monoclonal anti-Lamin A/C (JoL3)	Santa Cruz Biotechnology sc-56140
goat polyclonal anti-actin (I-19)	Santa Cruz Biotechnology sc-1616
donkey anti-goat IgG HRP conjugated	Santa Cruz Biotechnology sc-2020
goat anti-rabbit IgG (H+L)-HRP conjugated	Bio-Rad #1706515
goat anti-mouse IgG (H+L)-HRP conjugated	Bio-Rad #1706516
ANTIBODIES FOR IMMUNOISTOCHEMISTRY	**SOURSE and #catalogue**
rabbit polyclonal anti-phospho-Histone H3 (ser10)	Cell Signaling Technology #9701
mouse monoclonal anti-c-Abl (8E9)	Santa Cruz Biotechnology sc-56887

rabbit polyclonal anti-NIK (H-248)	Santa Cruz Biotechnology sc-7211
Biotinylated goat anti-mouse antibody	Vector Laboratories BA-9200
biotinylated goat anti-rabbit antibody	Vector Laboratories BA-1000
ANTIBODIES FOR IMMUNOFLUORESCENCE	**SOURSE and #catalogue**
mouse monoclonal anti-c-Abl (8E9)	Santa Cruz Biotechnology sc-56887
Goat anti-mouse IgG (H+L) Alexa Fluor 594	Invitrogen A-11032

Western blot

Proteins from whole cell lysates and nuclear fractions were quantified by Bradford assay and separated by SDS-PAGE and analyzed by Western blotting with the antibodies reported in the table above.

The interaction between NIK, c-Abl and STAT3 was evaluated by co-immunoprecipitation analysis by using ExactaCruz kits (Santa Cruz Biotechnology, Santa Cruz, CA) as per manufacturer's instructions. For immunoprecipitation, the following antibodies were used: rabbit polyclonal anti-NIK, mouse monoclonal anti-c-Abl from Santa Cruz Biotechnology and rabbit polyclonal anti-STAT3 from by Cell Signaling Technology.

RNA extraction, cDNA preparation and Real Time RT-PCR (qPCR)

RNA was extracted from HMCLs using TRIzol® reagent (Fisher Molecular Biology, Rome, IT) and purified with the PureLink® RNA Mini Kit (Fisher Molecular Biology, Rome, IT). cDNA was prepared using the RevertAid First Strand cDNA Synthesis kit (Thermo Fisher Scientific, Waltham, MA) following the manufacturer's instructions. Quantitative real-time PCR was performed in duplicate with a DNA Engine Opticon 4 (MJ Research, Walthman, MA, USA). The following Taqman probes/primers were used: NIK: Hs00177695_m1; TRAF2: Hs00184192m1; GAPDH: Hs99999905_m1 (Applied Biosystems) and the TaqMan Fast Universal PCR Master Mix (Applied Biosystems). Data were normalized to human GAPDH, and mRNA levels of NIK and TRAF2 in HMCLs were calculated using the $2^{-\Delta\Delta CT}$ method, where $\Delta\Delta CT = \Delta CT$ target sample - ΔCT control sample, and plotted as m RNA relative fold change in comparison to control cells. Relative mRNA fold changes values comprised between 0.5 and 2 are considered not biologically relevant.

Animal studies

NOD-SCID mice were subcutaneously inoculated in the left flank with 10^7 RPMI-8226/R5 cells in 200µL of PBS. NOD-SCID mice (n=5) injected with PBS alone were used as negative

controls. When tumors reached volumes of 250 mm^3, approximately 5-6 weeks after MM cell injection, mice were randomly assigned (12/group) to receive vehicle or drugs at various doses. Mice were treated with daily doses of pan-AKIs and/or Imatinib for two weeks. Both Pan-AKIs were formulated in 30% PEG300, 70% 50 mM sodium phosphate buffer pH3.3 (Sigma, St Louis, MO) and 50 mg/Kg of the two inhibitors were administered by intraperitoneal injection. Imatinib was dissolved in sterile water and administered by intraperitoneal injection at 50 mg/kg twice daily. Controls received a daily intraperitoneal injection of 30% PEG300, 70% 50 mM sodium phosphate buffer vehicle and/or PBS.

Mice were evaluated for weight loss, tumor mass and overall appearance every 2 days. Tumor size was measured in 2 dimensions using calipers, and tumor volume was calculated using the following formula: Volume = 0.5 x a x b^2, where "a" and "b" are the long and short diameter of the tumor, respectively. At different time point of drug treatment or when tumors reached 2 cm^3, animals were killed by cervical dislocation. Tumors were explanted 6-8 hours after the last drug administration. Immediately after euthanasia necropsies were performed and subcutaneous neoplasia (xenotransplantation) were collected, photographed and measured. Splanchnic organs from thoracic, peritoneal and cranial cavities as well as the right femur were also collected.

The tumor masses were submitted in part to Western blotting analysis, in part to morphological and immunohistochemical studies. Histomorphological investigations were performed on organs of splanchnic cavities as well as bone marrow collected from femur. To prepare lysates, tumor tissue was homogenized in lysis buffer and then processed as described above. For immunohistochemical studies, xenograft tumors were fixed overnight in paraformaldehyde followed by dehydration in graded ethanol.

Immunohistochemistry

Immunohistochemistry analysis of c-Abl was performed on HMCLs plated on a glass poly-L-lysinate slide by centrifugation with the use of the Shandon Cytospin 2 and fixed with 4% paraformaldehyde for 10 minutes. Cells were then permeabilized with PBS and 0.1% Triton X-100 for 10 minutes and incubate for 10 minutes in 0.1% hydrogen peroxide in PBS to quench endogenous peroxidase activity. Slides were incubated with mouse monoclonal anti-c-Abl antibody (dilution 1:100) for 60 minutes at room temperature.

Immunohistochemistry analysis of NIK, c-Abl and Phospho-Histone H3 (Ser10) was performed on formalin-fixed, paraffin-embedded tumor from treated mice and on cell pellets prepared from HMCLs. The expression of Caspase-3 was determined using the Kit of

Cell Signaling Technology (Signal Stain Cleaved Caspase-3 IHC #8120) according to manufacturer's protocol.

Formalin fixed sections (5 µm thick) were deparaffinized in xylene and rehydrated in ethanol; after antigen retrieval with citrate buffer pH6 for NIK, phospho-Histone H3 and cleaved caspase-3 antibodies or TRIS-EDTA pH9 for c-Abl antibody using microwave (3x5 minutes at 400 Watts), sections were incubated with Peroxidase Blocking Solution (3% H_2O_2 in PBS) for 12 minutes. For antibodies made in Rabbit, sections were incubate for 30 minutes in 5% normal goat serum in PBS; Slides were then incubated with anti-c-Abl antibody (dilution 1:100) or with anti-NIK antibody (dilution 1:150) or with anti-phospho-Histone H3 (dilution 1:200) overnight at 4°. After primary antibody labelling, the sections were rinsed with PBS and incubated with biotinylated secondary antibody in PBS for 30 minutes at room temperature. Sections were incubated in ABC-Peroxidase Solution (Vectastain) for 30 minutes at room temperature before peroxidase substrate solution. After counterstaining of nuclei with Mayer's hematoxylin, slides were dehydrated through ethanol and cleared in xylene.

Slides were examined with Nikon Eclipse E800 microscope (Nikon Corporation, Japan) using Nikon PLAN APO lenses. Sections were photographed at 10x, 20x, 40x and 100x (Nikon PLAN APO lenses) with Camera DIGITAL SIGHT DS-Fi1 (Nikon Corporation); pictures were acquired with DS Camera Control Unit DS-L2 (Nikon Corporation) and stored in USB device.

Immunofluorescence

Immunofluorescence analysis of c-Abl was performed on HMCLs plated on a glass poly-L-lysinate slide by centrifugation with Shandon Cytospin 2 and fixed with 4% paraformaldehyde in PBS for 10 minutes. Cells were then permeabilized in a solution of 0.01% Triton X-100 in PBS for 3 minutes and washed in three changes of PBS. Cells were treated for 30 minutes with 3% BSA in PBS to block unspecific binding sites and incubated with c-Abl antibody (1:200) overnight at 4°C in a dark chamber, followed by Alexa Fluor 594 goat anti-Mouse IgG antibody (2µg/ml), diluted with BSA 3% in PBS for 60 minutes at room temperature in a dark chamber. Nuclei were counterstained with DAPI; the slides were mounted with an aqueous mounting medium. Between each step the slides were washed with BSA 1% in PBS (three changes for 5 minutes each). Stained slides were viewed under a fluorescence microscope (Carl Zeiss Micro Imagine, Axio Observer.Z1, Germany) and were photographed at 63x magnification (-63X/0.75 LD Plan NeoFluar -63

X/1.4 Oil/DIC Plan Apo Chromat) with Axio Cam MRm (Carl Zeiss); pictures were acquired and analyzed with the AxioVision Rel. 4.8.2 software (Carl Zeiss).

The 100x images were captured using the Nikon Eclipse E600 Fluorescence Microscope (Nikon Corporation, Japan) with the Nikon Microscope 100x CFI Plan Fluor Oil Objective and were photographed with DS-Fi2 camera (Nikon); pictures were then acquired and analyzed with the NIS-Elements Microscope Imaging Software (Nikon).

Statistical analysis

For multiple comparisons a statistical analysis was performed using analysis of variance for repeated measurements followed by a Tukey-Kramer or Dunnet post-tests using JMP version 7.0 statistical software (SAS Institute, Cary, NC). The P values are shown in figure legends.

The Chou-Talalay method and Calcusyn software (Biosoft, Ferguson, MO) were used to assess synergistic or additive or antagonist effects of combined therapies. The mean combination index (CI) values of the combination NIK inhibitor plus pan-AKIs and Nilotinib plus pan-AKIs are summarized in supplemental tables S1 and S3.

Survival curves were derived by the Kaplan-Meier method and compared using the log-rank test, and P values for the log rank statistic were adjusted for multiple testing by the Bonferroni method (6 groups, 15 pairwise comparisons) using JMP software.

Supplemental References

1. Harrington EA, Bebbington D, Moore J, et al. VX-680, a potent and selective small-molecule inhibitor of the Aurora kinases, suppresses tumor growth in vivo. *Nat Med*. 2004;10(3):262-267

2. Soncini C, Carpinelli P, Gianellini L, et al. PHA-680632, a novel Aurora kinase inhibitor with potent antitumoral activity. *Clin Cancer Res*. 2006; 12(13):4080-4089..

3. Katayama H, Sen S. Aurora kinase inhibitors as anticancer molecules. *Biochim Biophys Acta* 2010;1799(10-12):829-839

4. ClinicalTrials.gov. Available from: https://clinicaltrials.gov/ct2/show/NCT00872300.

5. ClinicalTrials.gov. Available from: https://clinicaltrials.gov/ct2/show/NCT00766324.

6. Payton M, Bush TL, Chung G, et al. Preclinical evaluation of AMG 900, a novel potent and highly selective pan-aurora kinase inhibitor with activity in taxane-resistant tumor cell lines. *Cancer Res*. 2010;70(23):9846-9854.

7. Lapenna S, Giordano A (2009) Cell cycle kinases as therapeutic targets for cancer. *Nat Rev Drug Discov* 8(7):547-566.

8. Kantarjian HM, Schuster MW, Jain N, et al. A phase 1 study of AMG 900, an orally administered pan-aurora kinase inhibitor, in adult patients with acute myeloid leukemia. *Am J Hematol*. 2017;92(7):660-667.

Table S1. Combination index (CI) values of the combination NIK inhibitor and pan-AKIs.

HMCL	COMBINATION	RATIO (μM)	MEAN COMBINATION INDEX (CI)	SD
OPM-2	NIK-in+MK	10:2	0.420653333	0.111817226
RPMI-8226	NIK-in+PHA	10:1	0.297306667	0.230820087
RPMI-8226/R5	NIK-in+MK	10:1	0.28196	0.183394748
U266	NIK-in+PHA	10:0.5	0.12136	0.06582217
JJN3	NIK-in+MK	10:0.5	0.255526667	0.065582469

HMCLs were treated sequentially with escalating doses of the NIK inhibitor isoquinoline-1,3 (2H,4H)-dione (NIK-in) (1-20 μM) for 3 hours and subsequently with MK-0457 (0.1-1 μM) or PHA-680632 (0.1-2 μM) alone or in combination with the NIK inhibitor at fixed ratios indicated in table. After 48 hours, cell death was measured by annexin V labeling and the Combination Index values (CI) were calculated using the Chou-Talalay method and Calcusyn software. Mean CI ± SD was estimated from CI at ED50, ED75 and ED90 values of the combination NIK-in+pan-AKIs. CI values less than 1.0 indicate synergism, CI values equal to 1.0 indicate additive effect and CI values more than 1.0 indicate an antagonistic effect.

Table S2. Clinical characteristics of the MM patients.

	AGE	PATIENT STAGE	% BM PLASMA CELLS	STATE OF DESEASE	THERAPY at RELAPSE
SAMPLE#1	70	IIIB ISS3	>90	5th relapse	LEN/DEX
SAMPLE#2	68	IIIB ISS3	7	1st relapse	LEN/DEX
SAMPLE#3	72	IIIA ISS2	34	1st relapse	LEN/DEX
SAMPLE#4	64	IIIB ISS2	3	1st relapse	VCD
SAMPLE#5	61	IIIA ISS2	40	3rd relapse	DARATUMUMAB
SAMPLE#6	73	IIIB ISS2	>90	1st relapse	VEL/DEX
SAMPLE#7	72	IIIA ISS2	54	1st diagnosis	KRD
SAMPLE#8	58	IIIA ISS2	15	1st diagnosis	VTD
SAMPLE#9	54	IIA ISS1	5	1st diagnosis	VTD
SAMPLE#10	80	IIIA ISS3	80	1st diagnosis	-
SAMPLE#11	69	IIA ISS2	45	2nd relapse	LEN/DEX
SAMPLE#12	73	IIIA ISS2	40	4th relapse	BENDA/PRED
SAMPLE#13	86	NR	60	1st relapse	LEN/DEX

Primary CD138+ MM cells were isolated from BM aspiration of MM patients at the diagnosis or relapse, and were treated in vitro with pan-AKIs in combination with NIK inhibitor, or PIM1/2 inhibitor or Imatinib as described in text. LEN/DEX indicates Lenalidomide plus Dexamethasone; VCD indicates Bortezomib, Cyclophosphamide and Dexamethasone; VEL/DEX indicates Bortezomib and Dexamethasone; KRD indicates Carfilzomib, Lenalidomide and Dexamethasone; VTD indicates Bortezomib, Thalidomide and Dexamethasone; BENDA/PRED indicates Bendamustine and Prednisone.

Table S3. Combination index (CI) values of the combination Nilotinib and pan-AKIs.

HMCL	COMBINATION	RATIO (μM)	MEAN COMBINATION INDEX (CI)	SD
OPM-2	NILOTINIB+AMG	1: 0.01	0.10681	0.036421945
	NILOTINIB+MK	1:0.1	0.073526667	0.042373615
RPMI-8226	NILOTINIB+AMG	1: 0.01	0.039516667	0.003002405
	NILOTINIB+MK	1:0.1	0.007176667	0.007899711
RPMI-8226-NIK	NILOTINIB+AMG	1: 0.01	0.00378	0.005035901
	NILOTINIB+PHA	1:0.5	0.002616667	0.003661562
RPMI-8226/R5	NILOTINIB+AMG	1: 0.01	0.02094	0.02049397
	NILOTINIB+MK	1:0.1	0.027556667	0.033588591
U266	NILOTINIB+AMG	1: 0.01	1,05699	0,120464715
	NILOTINIB+MK	1:0.1	1,52271	0,24715798
JJN3	NILOTINIB+AMG	1: 0.01	0.083423333	0.030959665
	NILOTINIB+MK	1:0.1	0.21146	0.059702036

HMCLs were treated sequentially with escalating doses of the Tyrosine kinase inhibitor Nilotinib (0.5-20 μM) for 3 hours and subsequently with the Aurora Kinase inhibitor AMG-900 (0.005-0.1 μM) or MK-0457 (0.05-1 μM) or PHA-680632 (0.1-2 μM) alone or in combination with Nilotinib at fixed ratios indicated in table. After 48 hours, cell death was measured by annexin V labeling and the Combination Index (CI) values were calculated using the Chou-Talalay method and Calcusyn software. Mean CI ± SD was estimated from CI at ED50, ED75 and ED90 values of the combination Nilotinib+pan-AKIs. CI values less than 1.0 indicate synergism, CI values equal to 1.0 indicate additive effect and CI values more than 1.0 indicate an antagonistic effect.

Table S4. Mean survival time of NOD-SCID mice.

GROUP	MEDIAN SURVIVAL	CONFIDENCE INTERVAL (CI)<95%	CONFIDENCE INTERVAL (CI)>95%
VEHICLE	15,5	12	18
MK-0457	29	24	32
PHA-680632	26,5	22	34
IMATINIB	16,5	12	21
IMATINIB+MK	58,5	40	69
IMATINIB+PHA	53,5	43	77

NOD-SCID mice xenografted with RPMI-8226/R5 cells were randomly assigned (n=8/group) to receive vehicle alone, MK-0457 (50 mg/kg), PHA-680632 (50 mg/kg), Imatinib (50 mg/kg twice daily), or the combination Imatinib/MK-0457 or Imatinib/PHA-680632 for two weeks. The median survival time and confidence interval were estimated from the Kaplan-Meier survival curve evaluated from the first day of treatment until death or sacrifice.

Figure S1

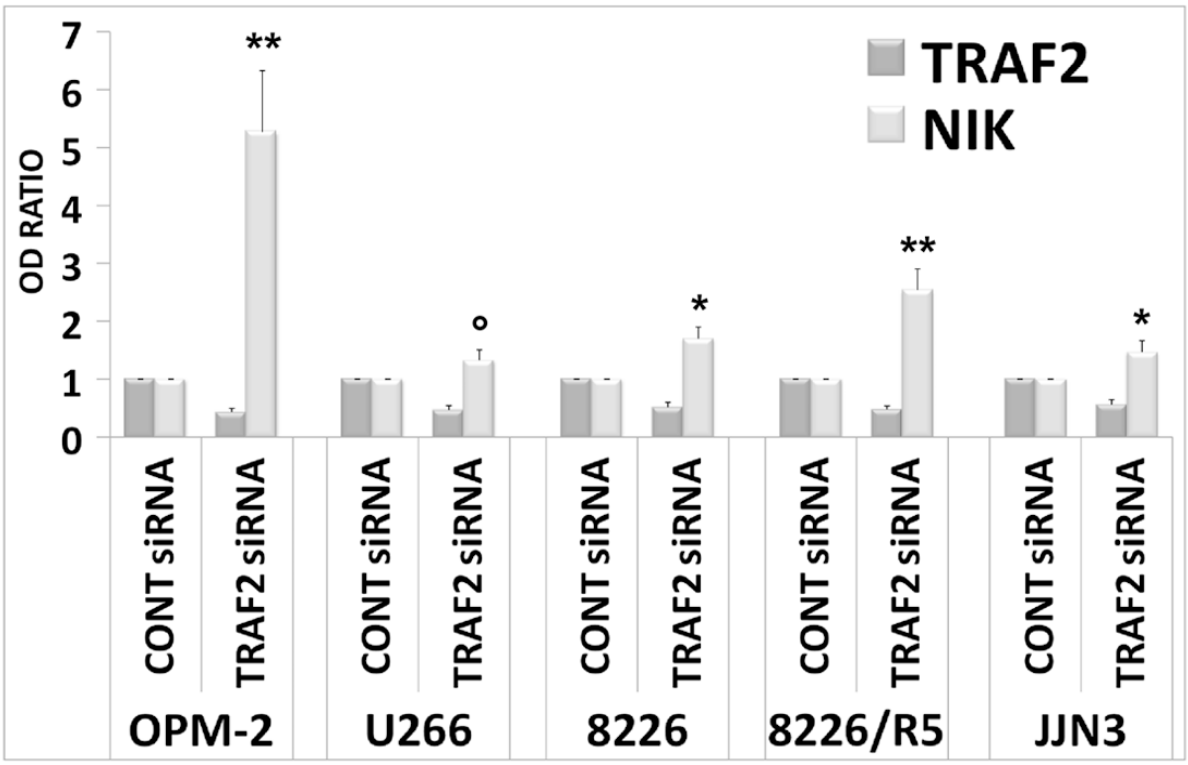

siRNA silencing of TRAF2 induces NIK expression. Histogram represents the densitometric analysis of TRAF2 siRNA western results showed in Figure 1D in the manuscript: TRAF2 and NIK bands were evaluated by densitometric scanning, normalized to actin expression, and expressed relative to the value obtained in the untreated control, which was taken as 1, and is shown under each lane. Histogram represents the mean ± SD of three independent experiments. (°P< .05, *P< .01, **P< .005 vs. Control siRNA; Dunnett and Tukey-Kramer tests).

Figure S2 A

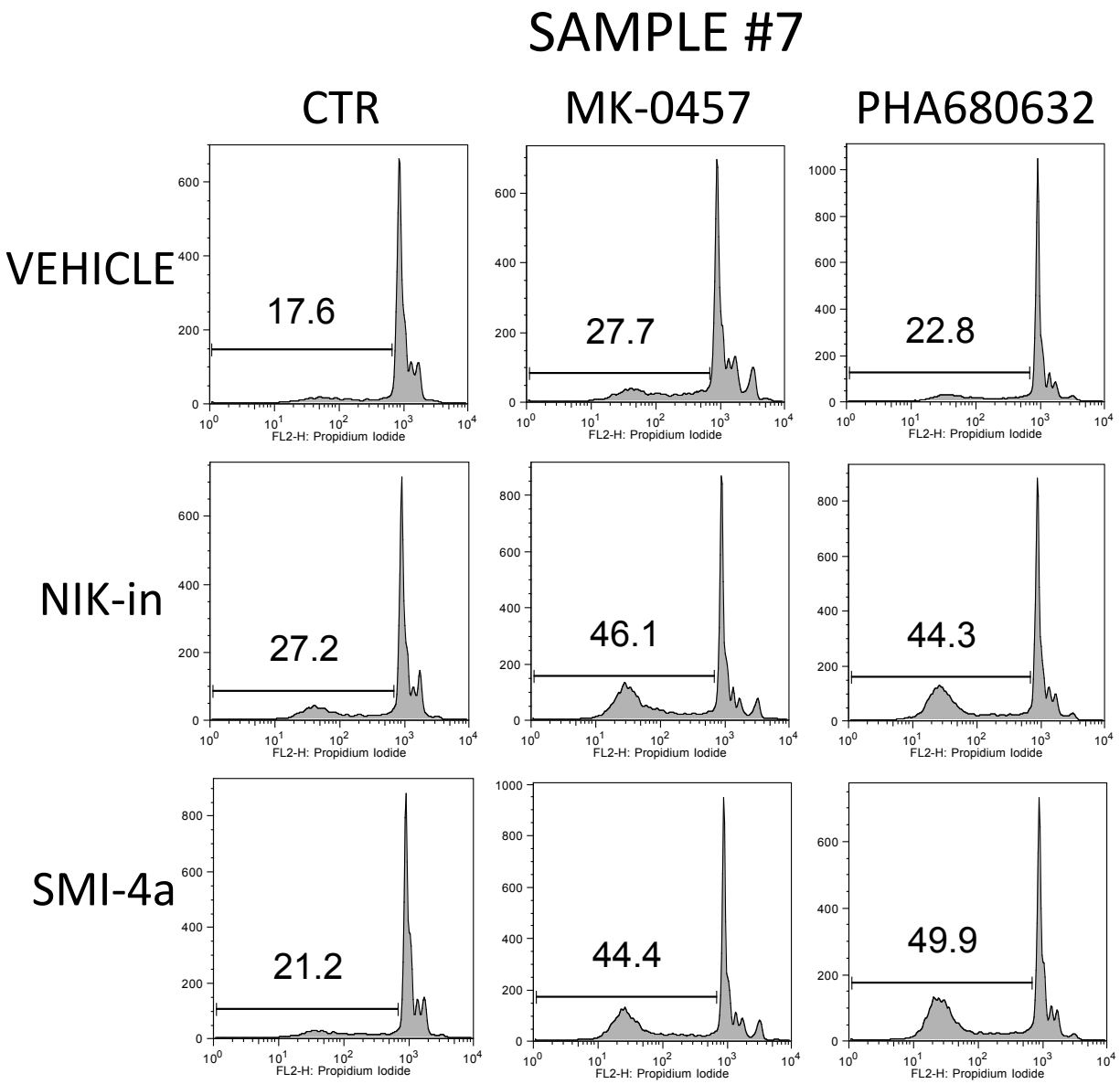
SAMPLE #7
CTR
MK-0457
PHA680632
VEHICLE
NIK-in
SMI-4a
17.6
27.7
22.8
27.2
46.1
44.3
21.2
44.4
49.9
FL2-H: Propidium Iodide

Figure S2 B

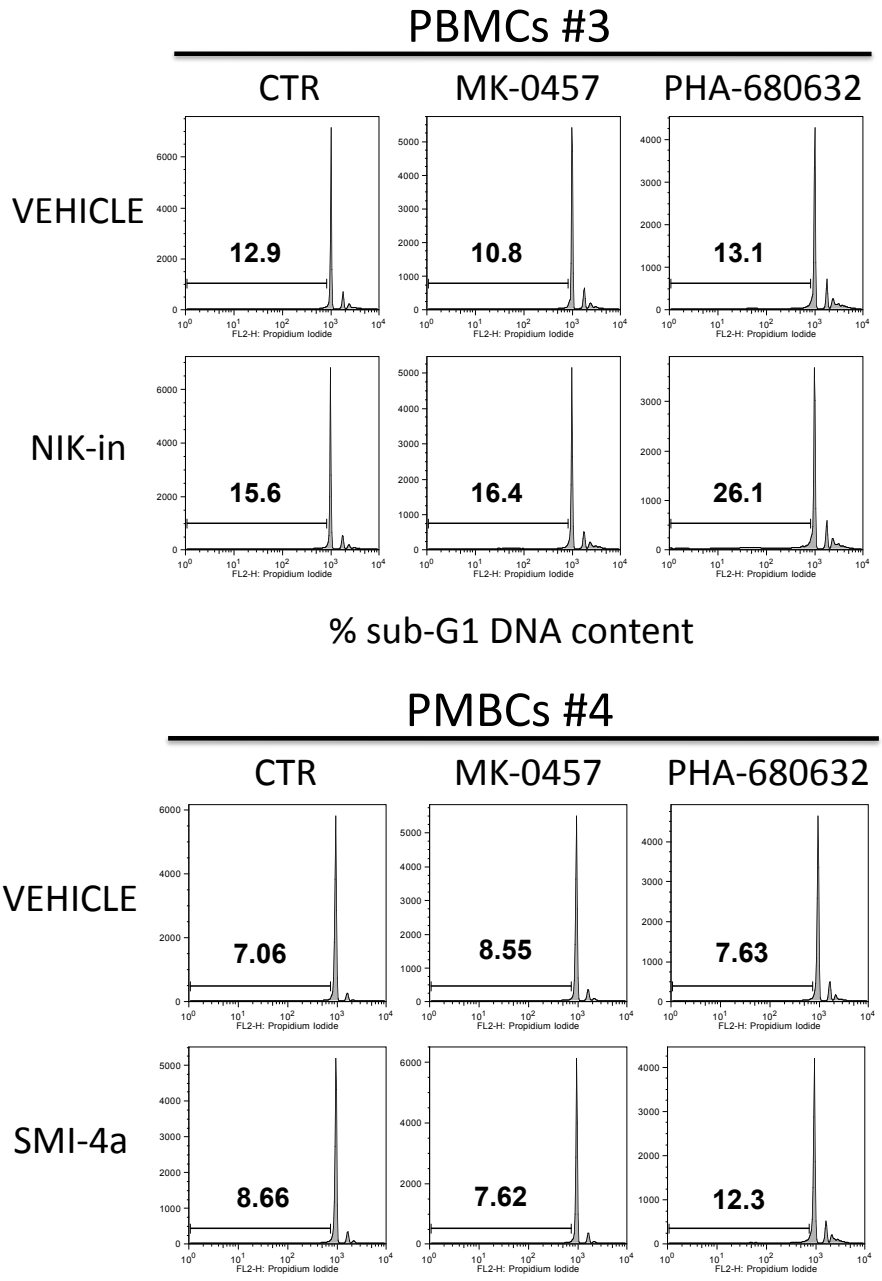

Representative flow cytometry data of primary MM samples **(A)** and PBMCs **(B)** from healthy donors. CD138-purified plasma cells from a patient (SAMPLE #7) with MM and PBMCs from healthy subjects (PBMCs #3 and #4) were incubated with the NIK inhibitor (NIK-in) at 10 μM or with the pan-PIM kinase inhibitor (SMI-4a) at 10 μM for 3 hours and then were treated with MK-0457 (0.4μM) or PHA-680632 (1μM). MM sample was cultured in presence of human bone marrow-derived stromal cell line HS-5 in a 5:1 ratio. After 48h apoptosis was detected by measurement of sub-G1 DNA content.

Figure S3

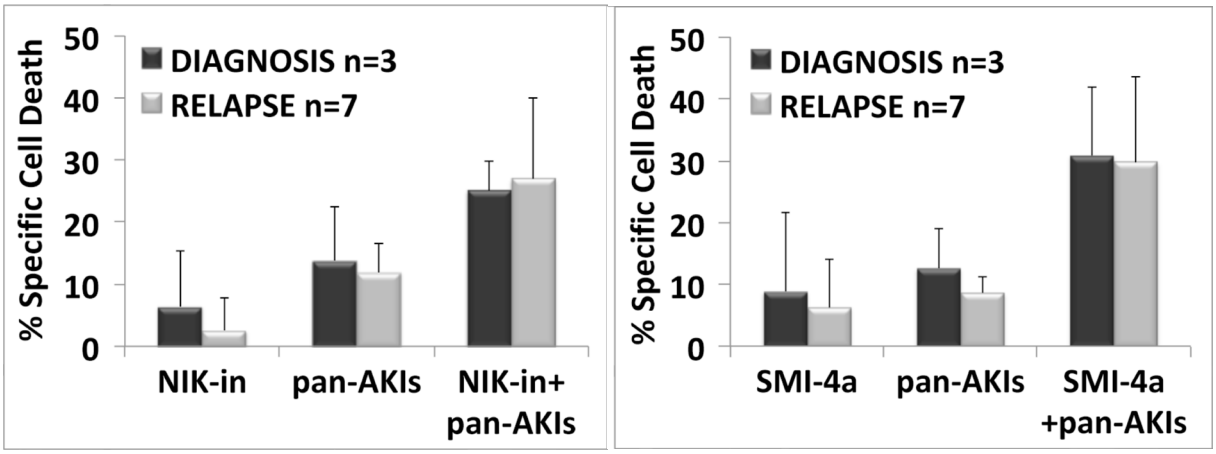

CD138-purified plasma cells from patients with MM seeded in presence of HS-5 cells were incubated with the NIK inhibitor (NIK-in) at 10 μM or with the pan-PIM kinase inhibitor (SMI-4a) at 10 μM for 3 h and then were treated with MK-0457 (0.4μM) or PHA-680632 (1μM). After 24h cell death was measured by annexin-V staining or sub-G1 DNA content. Because of heterogeneous levels of basal cell death, the data of all primary samples tested are expressed as % of specific cell death with the formula % Specific cell death = 100 x (induced cell death−basal cell death)/(100−basal cell death). Values in the histograms represent means ± SD of newly diagnosed (n=3) and relapsed (n=7) MM samples.

Figure S4 A

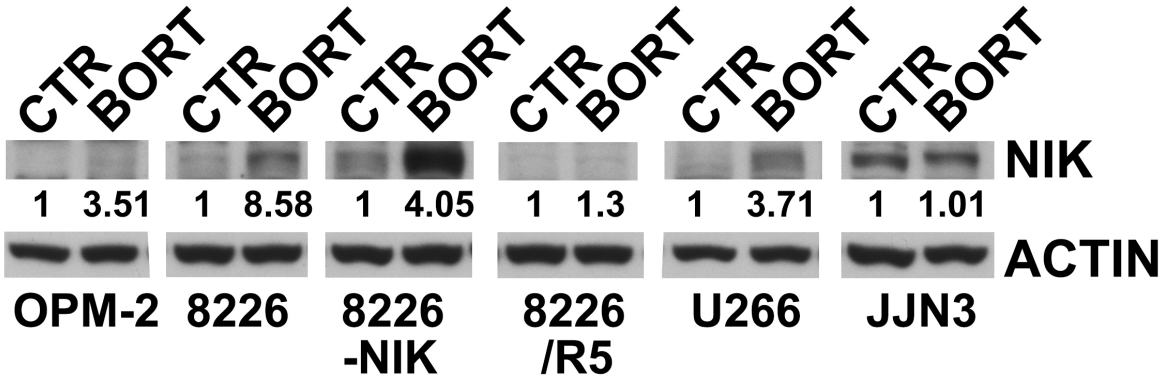

Figure S4 B

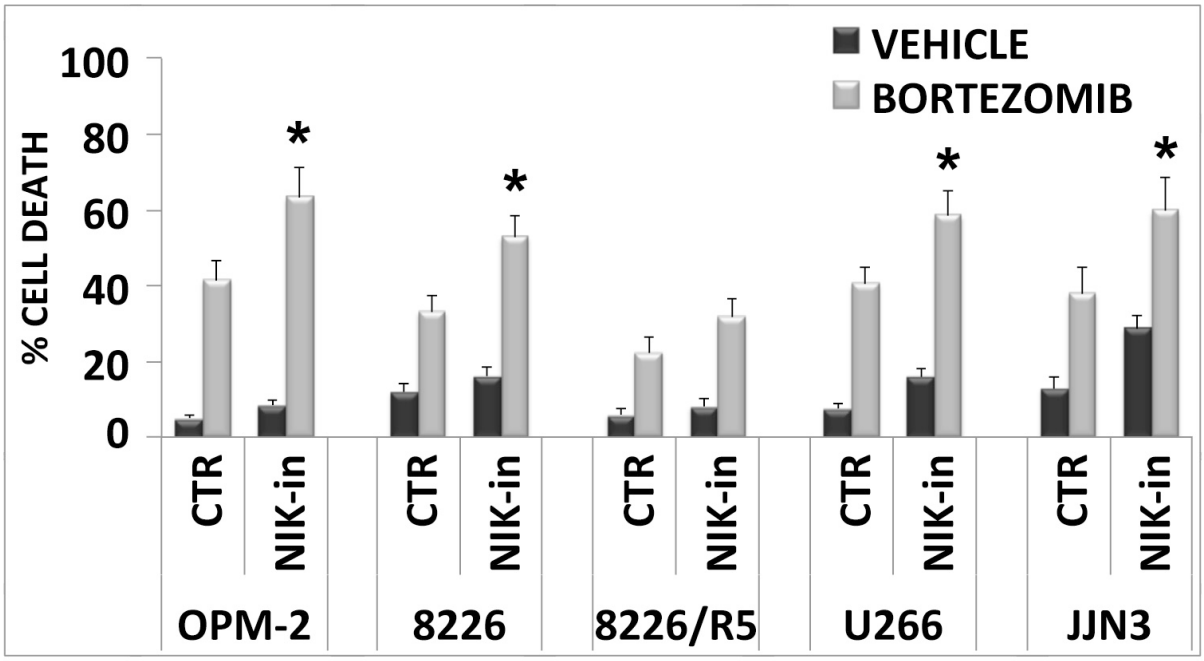

(A) HMCLs were incubated with Bortezomib (BORT) at 5 nM for OPM-2, 8226, U266 and JJN3 or at 10 nM for 8226/R5. After 24h HMCLs were subjected to western blot analysis to monitor the expression of NIK and actin as loading control. Bands were subjected to densitometric scanning and NIK expression was normalized to actin levels. NIK level under untreated control condition was set as 1 for comparison. **(B)** HMCLs were incubated with the NIK inhibitor (NIK-in) at 10 µM and after 3h HMCLs were treated with Bortezomib at 5 nM for OPM-2, 8226, U266 and JJN3 or at 10 nM for 8226/R5. After 48h, cell death was measured by annexin-V labeling. Values represent means ± SD of 3 independent experiments (*P< .05, Tukey-Kramer's test).

Figure S5

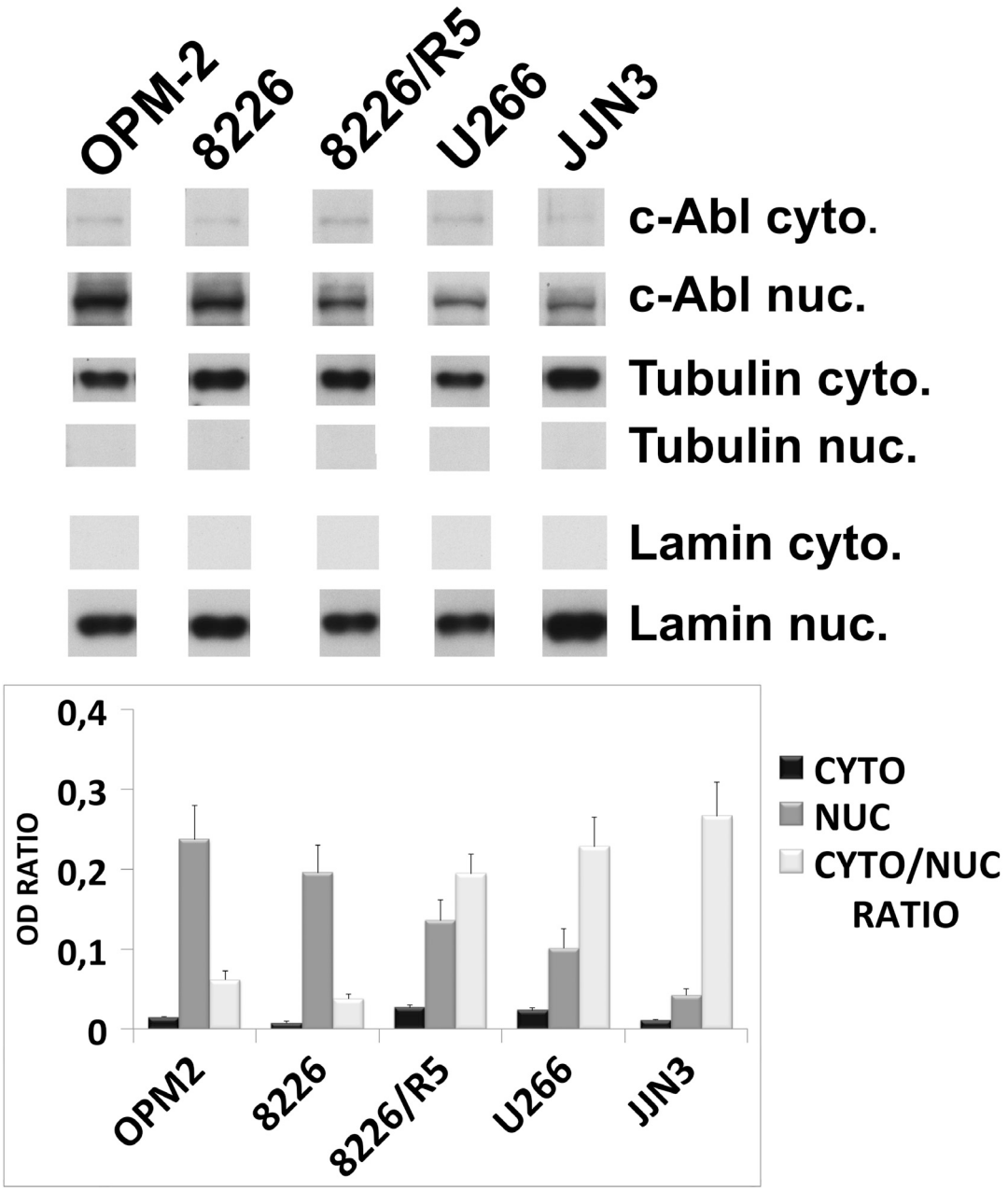

HMCLs were seeded at a density of $2x10^5$ cells/mL and after 24 hours cytoplasmic and nuclear extracts were prepared using the Active Motif's Nuclear Extract Kit. Equal amount of Cytoplasmic (cyto) and nuclear (nucl) cell lysates (10 µg) were loaded on the same gel and probed by immunoblotting for c-Abl, β-tubulin and lamin as loading control of cytoplasmic and nuclear fraction respectively. Nonadjacent bands from the same blot with an identical exposure were juxtaposed to facilitate comparisons. Bands were then subjected to densitometric scanning: cytoplasmic and nuclear blots were normalized to total tubulin and lamin respectively. The relative quantification of cytoplasmic (cyto) and nuclear (nuc) c-Abl bands is reported in histogram. The ratio of cytoplasmic to nuclear c-Abl protein expression (Cyto/Nuc) is shown.

Figure S6 A

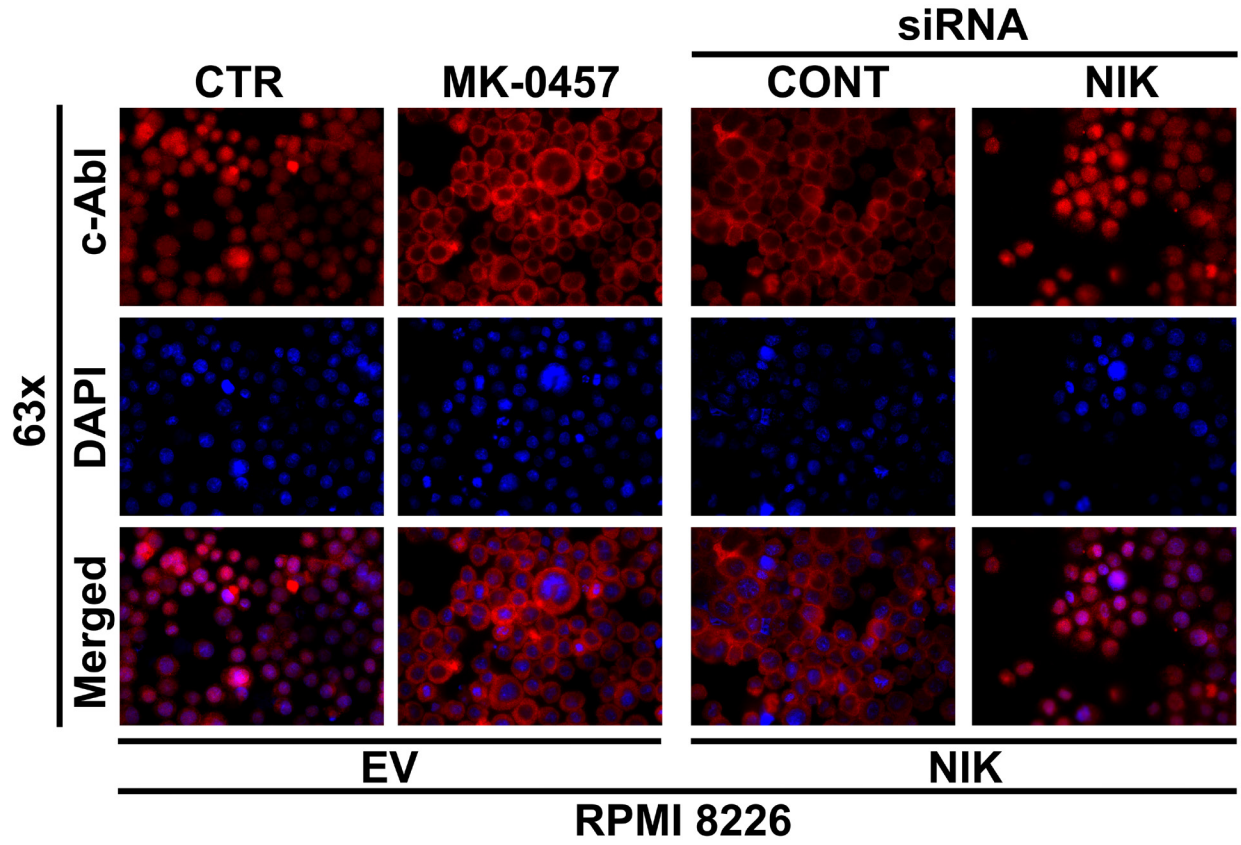

Figure S6 B

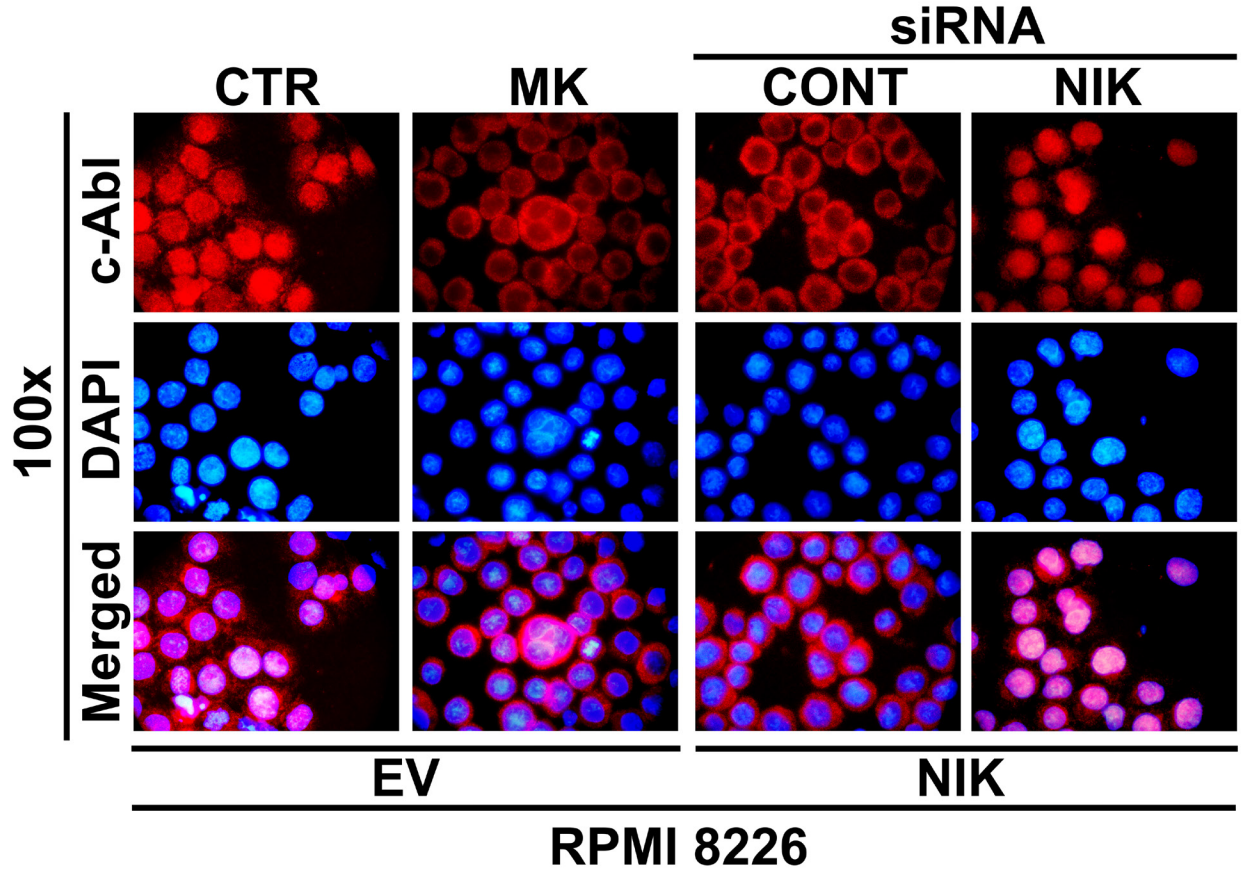

Stable clones of RPMI-8226 transfected with empty vector (EV) were treated with MK-0457 (0.4μM) and RPMI-8226 cells expressing NIK (NIK) were electroporated with non-specific control siRNA (CONT) or with NIK siRNA. After 24h cells were harvested for cytospins for immunofluorescence staining of c-Abl (Red) and DAPI (blue) for nuclear staining. The merged images represent merging of the c-Abl and DAPI images. The microphotographs shown in panel **(A)** (63x original magnification) and in **(B)** (100x original magnification) are representative of similar observation in 3 independent experiments.

Figure S7 A

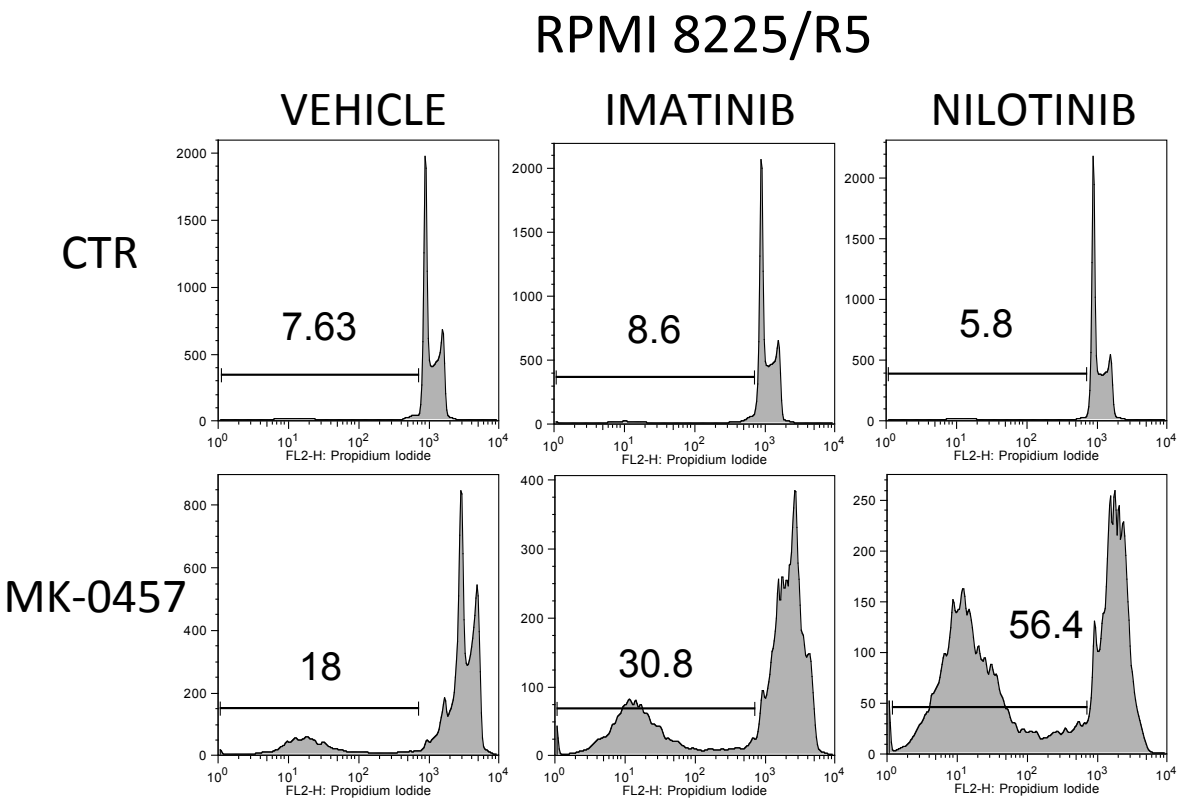

Figure S7 B

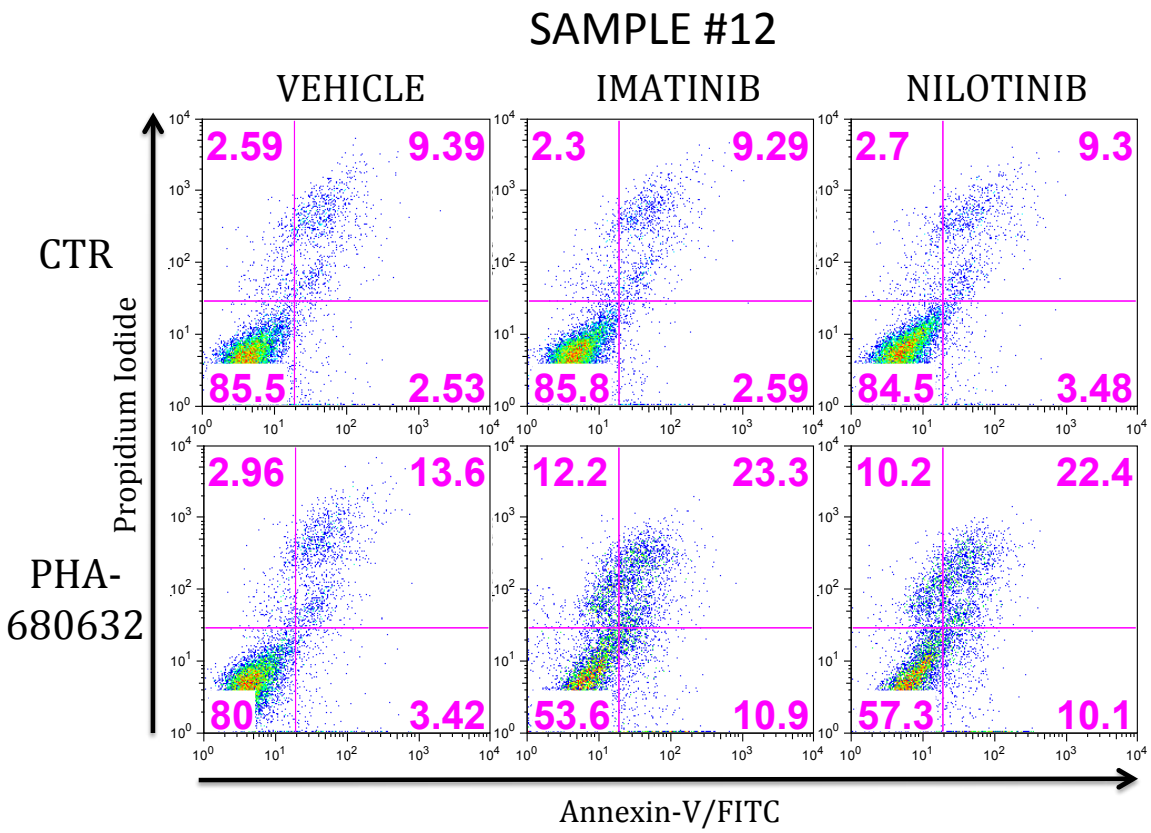

Figure S7 C

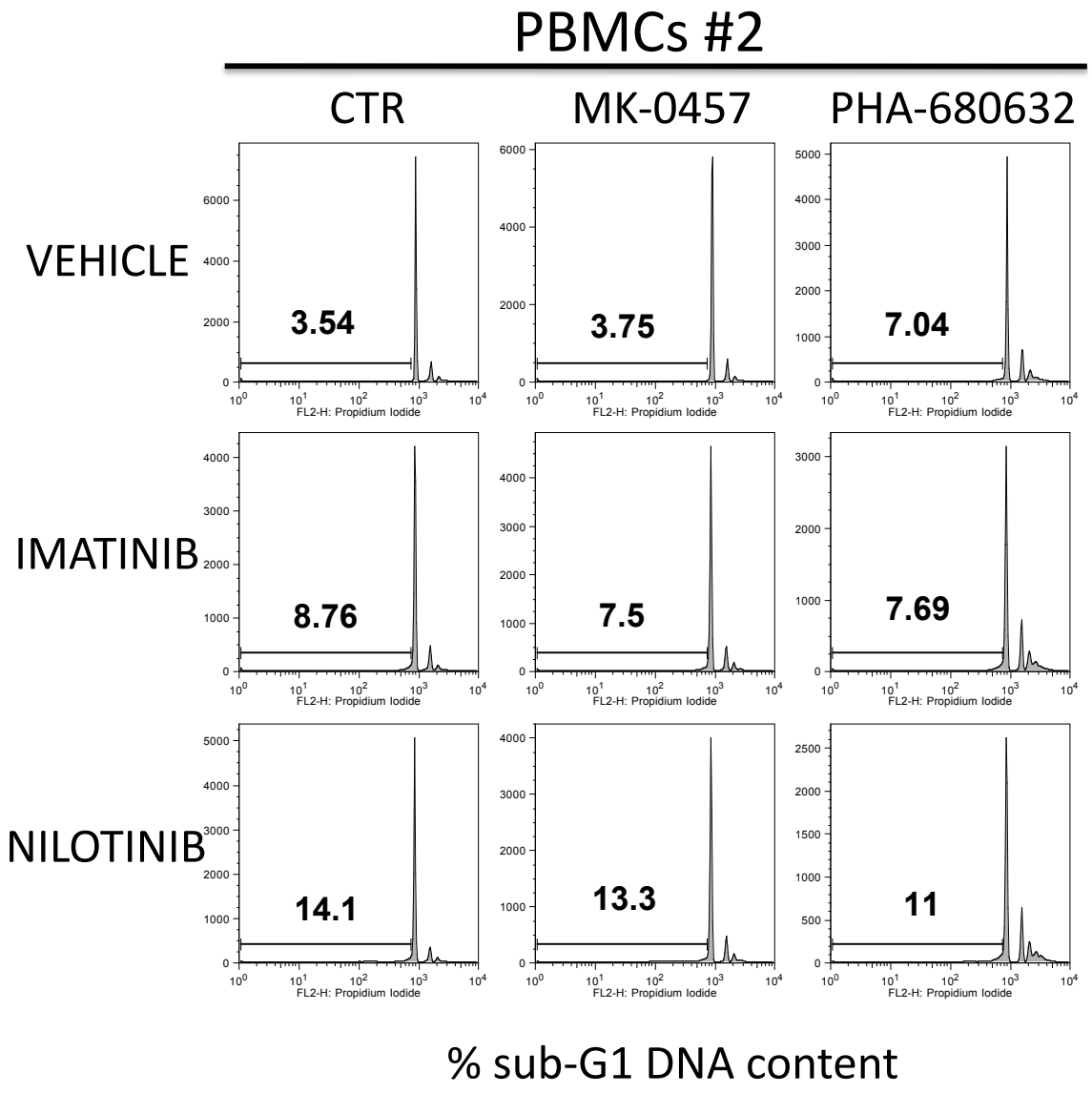

Flow cytometry data of representative experiments. RPMI-8226/R5 cells **(A)** as well as primary MM cells (Sample#12) **(B)** and normal PBMCs (Sample #2) **(C)** were incubated with Imatinib or Nilotinib at 2 μM for 3 hours, and then were treated with MK-0457 (0.4μM) or PHA-680632 (1μM). After 48h cell death was measured by sub-G1 DNA content for 8226/R5 **(A)**, and normal PBMCs (SAMPLE #2) **(C)** or annexin-V staining for primary MM cells (Sample#12) **(B)**.

Figure S8

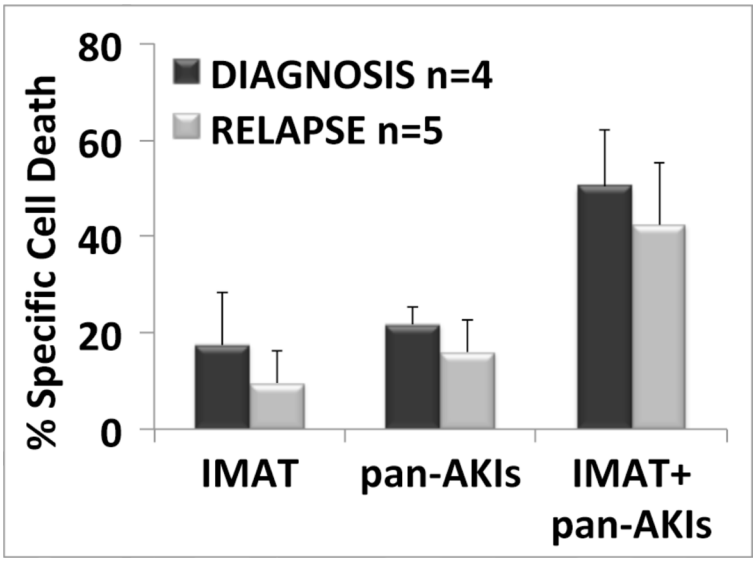

CD138-purified plasma cells from 9 patients with MM seeded in presence of HS-5 cells were incubated with Imatinib or Nilotinib at 2 μM for 3 h plus MK-0457 (0.4μM) or PHA-680632 (1μM). After 24h cell death was measured by annexin-V staining or sub-G1 DNA content. Because of heterogeneous levels of basal cell death, the data of all primary samples tested are expressed as % of specific cell death with the formula % Specific cell death = 100 x (induced cell death−basal cell death)/(100−basal cell death). Values in the histograms represent means ± SD of newly diagnosed (n=4) and relapsed (n=5) MM samples.

Figure S9

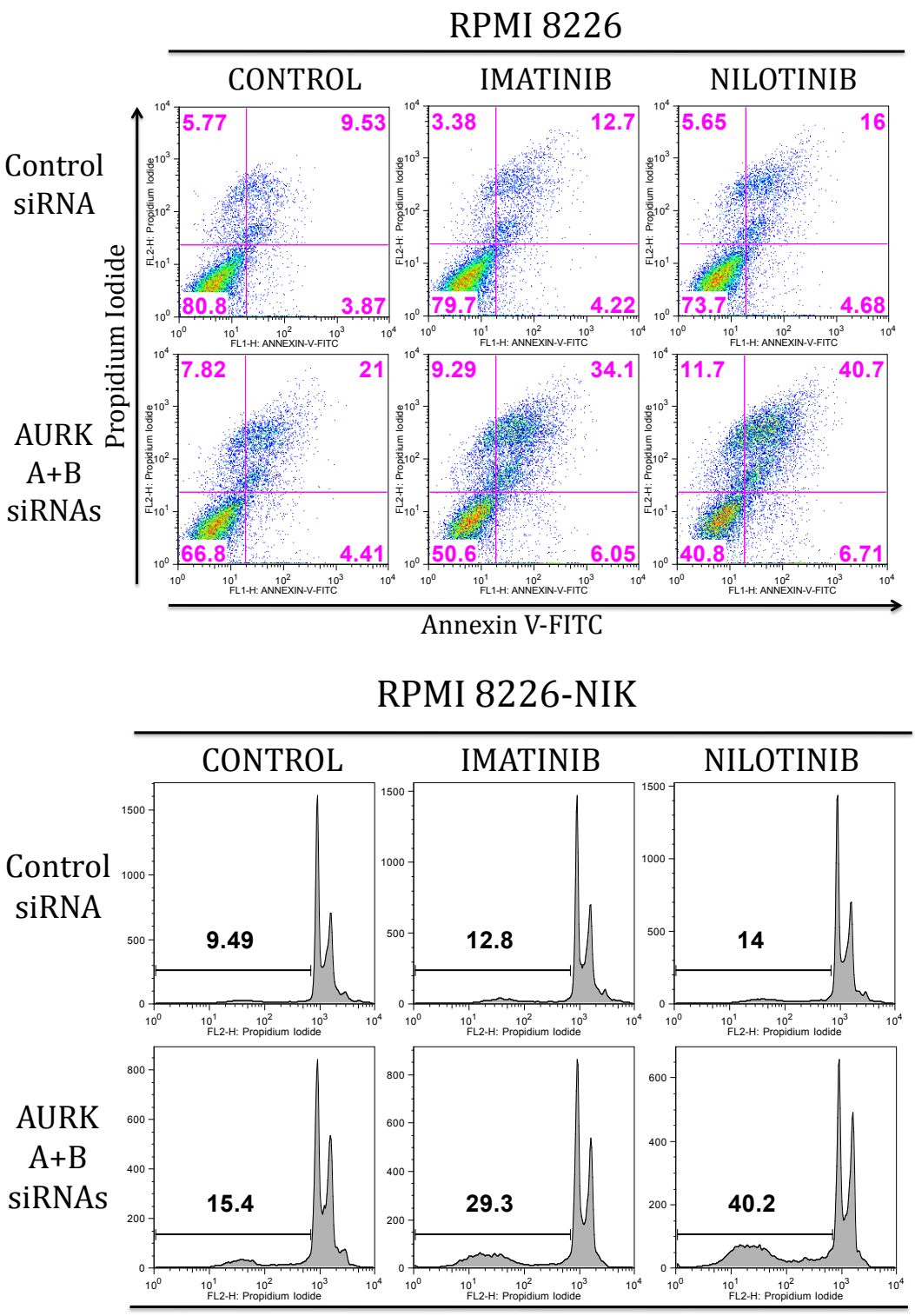

HMCLs were transfected with siRNA against Aurora A and Aurora B (AURK A+B) or control siRNA (Cont). 24 hours after siRNA transfection HMCLs were treated with Imatinib and Nilotinib at 2 μM. Cell death was measured by sub-G1 DNA content or annexin-V staining. In figure are shown flow cytometry data of a representative experiment analyzed by Annexin-V staining (RPMI-8226) or sub-G1 DNA content (RPMI-8226-NIK) after 48h of treatment.

Figure S10 A

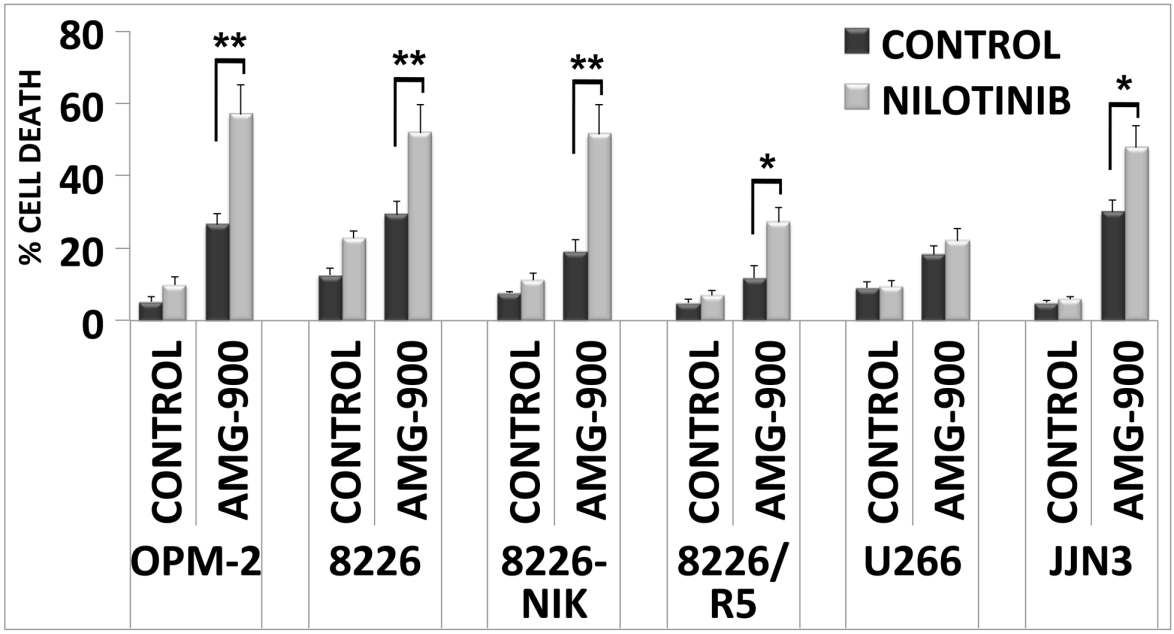

Figure S10 B

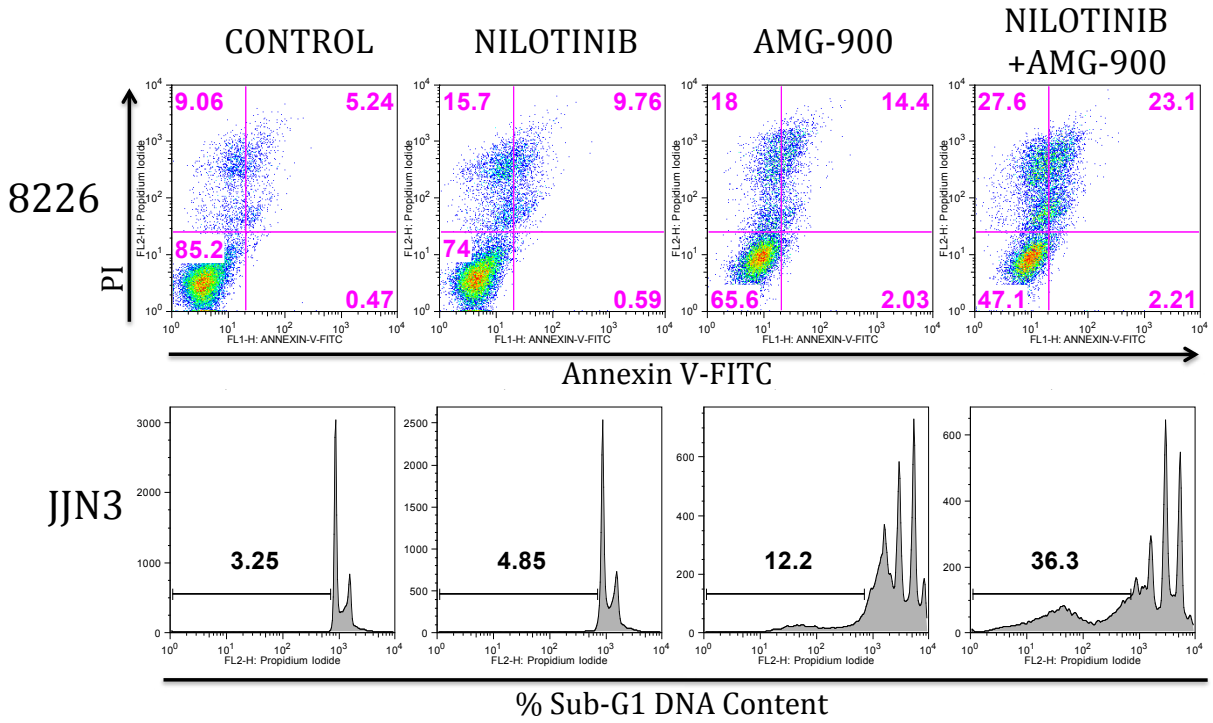

(A) HMCLs were incubated with Nilotinib at 2 µM for 3 hours, and then were treated with the Aurora Kinase Inhibitor AMG-900 at 40 nM. After 48h cell death was measured by annexin-V staining. Values represent means ± SD of four independent experiments. (*P< .05, **P< .01 vs. AMG-900 treatment; Dunnett test). **(B)** Flow cytometry data of a representative experiment analyzed by Annexin-V staining (8226) or sub-G1 DNA content (JJN3) after 48 hours of treatment.

Figure S11

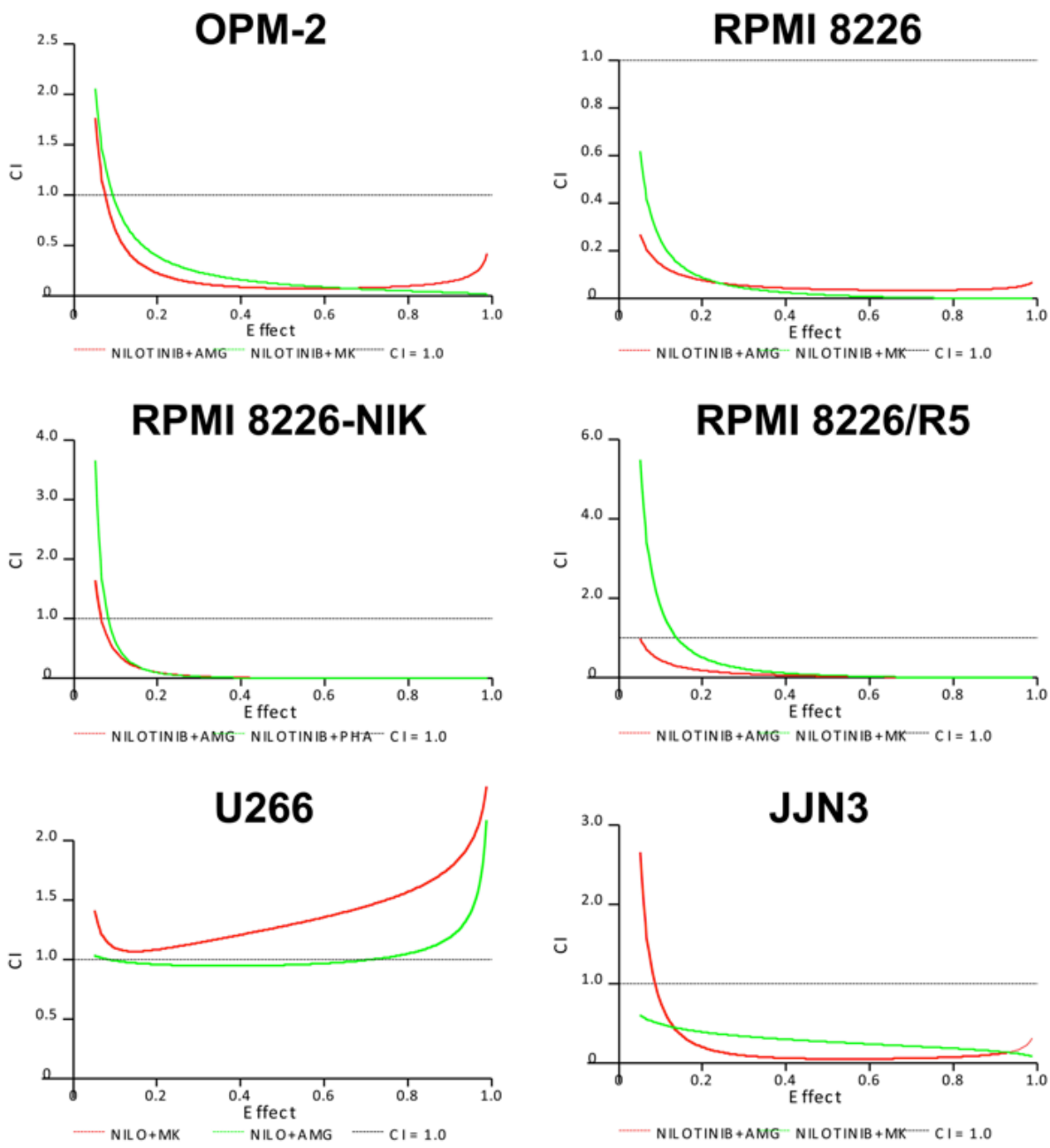

HMCLs were treated sequentially with escalating doses of the Tyrosine kinase inhibitor Nilotinib (0.5-20 µM) for 3 hours and subsequently with the Aurora Kinase inhibitor AMG-900 (5-100 µM) or MK-0457 (0.05-1 µM) or PHA-680632 (0.1-2 µM) alone or in combination with Nilotinib at a fixed ratio indicated in Supplemental Table S3. After 48 hours, cell death was measured by annexin V labeling and the isobologram plots were constructed. CI values less than 1.0 indicate synergism, CI values equal to 1.0 indicate additive effect and CI values more than 1.0 indicate an antagonistic effect.

Figure S12

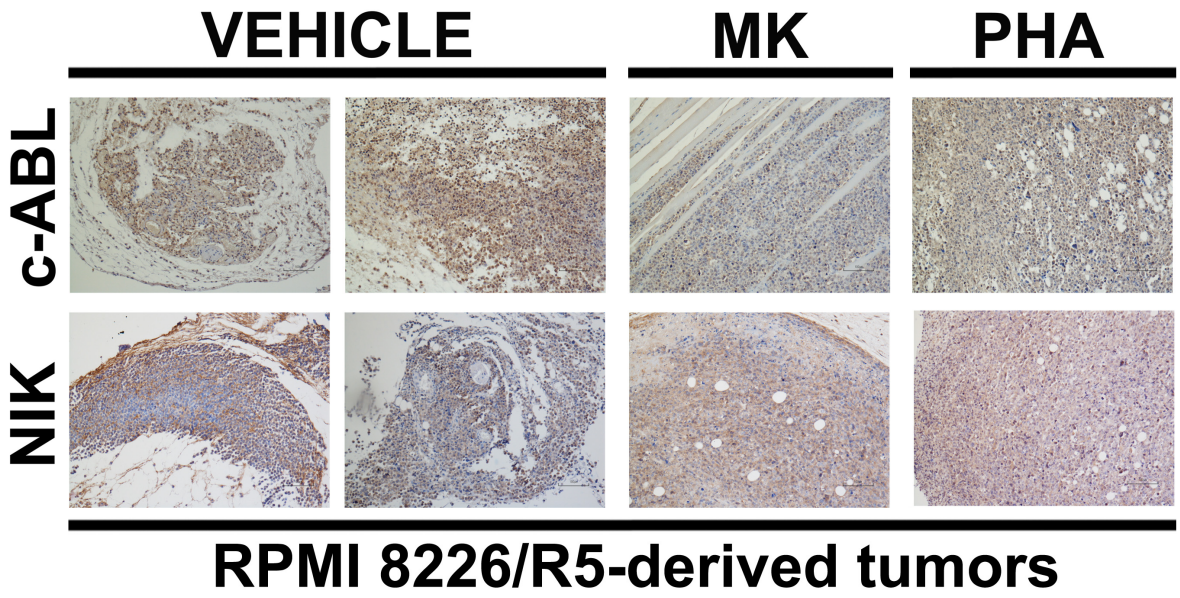

RPMI-8226/R5-derived tumors from vehicle or pan-AKIs treated NOD-SCID mice were formalin fixed paraffin embedded and analyzed by immunohistochemical analysis of c-Abl and NIK after 5 days of treatment. The microphotographs shown are representative of similar observation in 4 mice receiving the same treatment (10x original magnification).

Figure S13

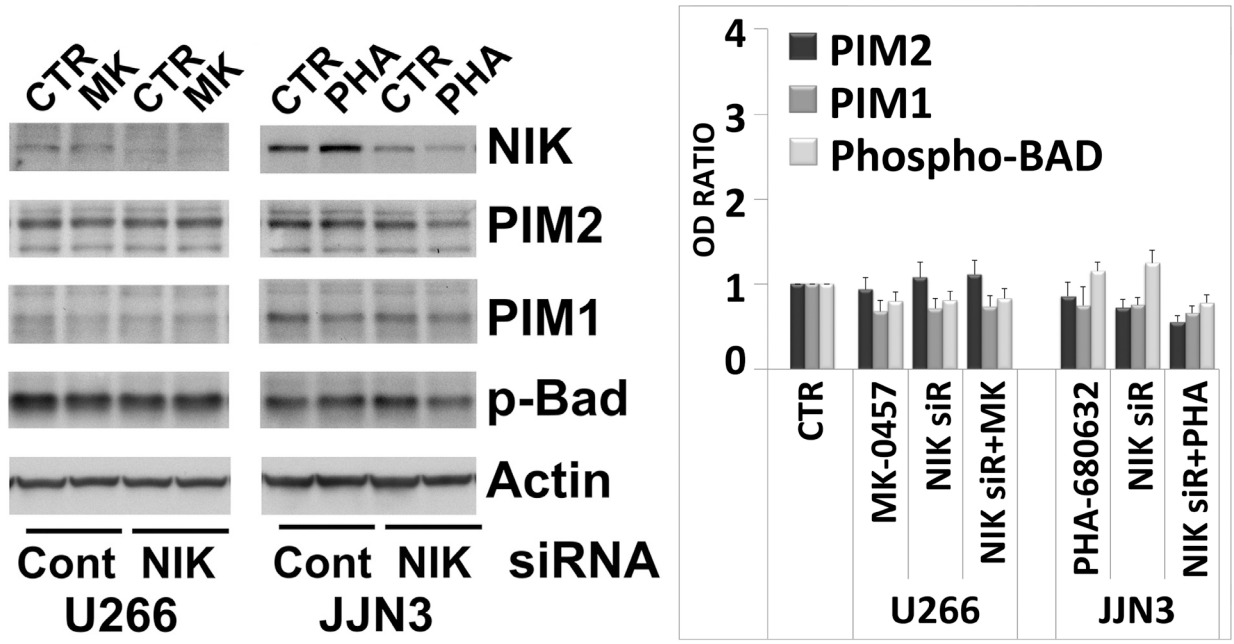

Western blot analysis of NIK, PIM2, PIM1, phospho-Bad (Ser112) and actin proteins in U266 and JJN3 cells transfected with NIK siRNA in presence or absence of MK-0457 (0.4μM) or PHA-680632 (1μM). All Western blotting results were evaluated by densitometric scanning and normalized to the untreated control set as 1. The histogram shows combined densitometric values of the 34, 37, and 40 kDa PIM2 bands. Histogram represents the mean ± SD of 3 independent experiments.

Figure S14

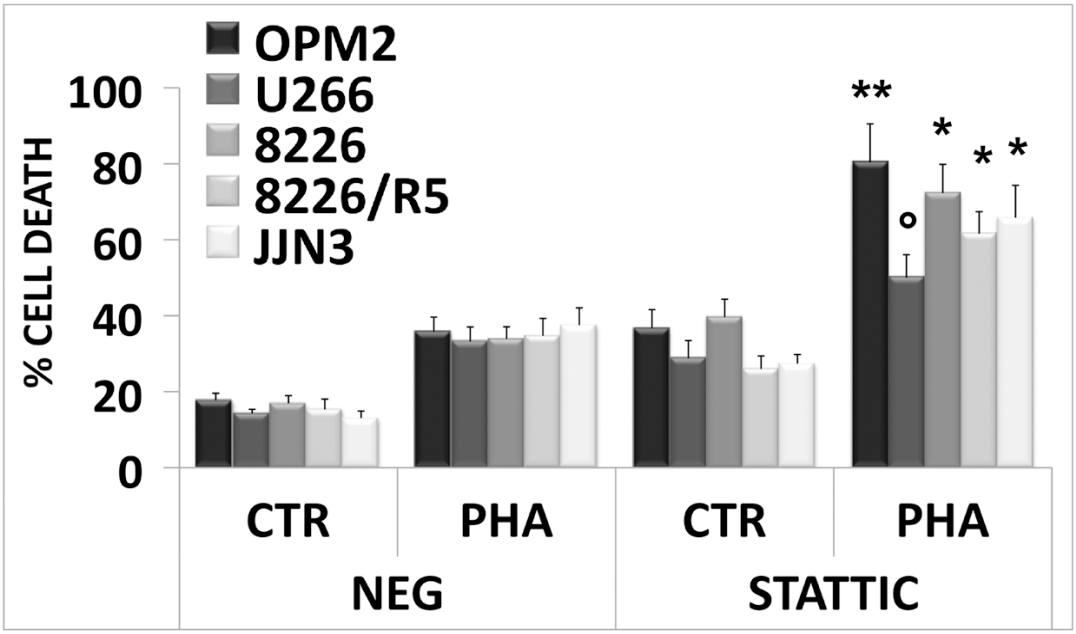

HMCLs were pre-incubated with the STAT3 inhibitory compound Stattic at 1 μM for 3 hours, and then were treated with PHA-680632 at 1μM. After 48 hours, cell death was measured by flow cytometry analysis of annexin V/PI staining. Values represent means ± SD of four independent experiments. (°P< .05, *P< .005, **P< .001 vs. either treatment alone; Dunnett and Tukey-Kramer tests).

Figure S15

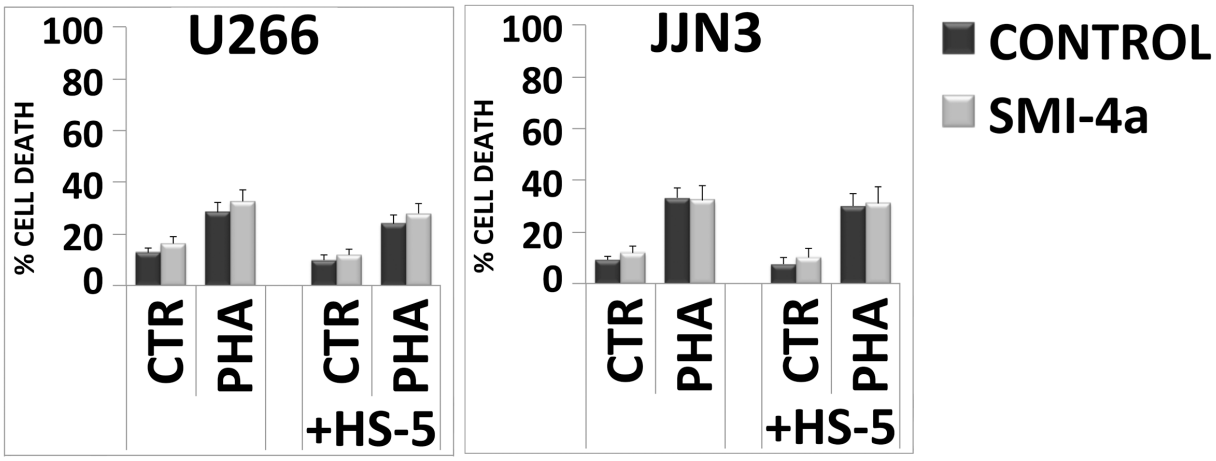

U266 and JJN3 cells were incubated with the pan-PIM kinase inhibitor (SMI-4a) at 10 μM for 3h, and then were treated with PHA-680632 (1μM) in absence or presence of HS-5 cells (+HS-5). After 48h cell death was measured by flow cytometry analysis of Annexin-V staining. Values represent means ± SD of 3 independent experiments.